Amperometric Batch Injection Analysis: Theoretical Aspects of Current Transients and Comparison with Wall-Jet Electrodes in Continuous Flow

Christopher M.A. Brett,[*+] *Ana Maria Oliveira Brett,*[*+] and *Lucian Costel Mitoseriu*[++]

[+] Departamento de Química, Universidade de Coimbra, 3049 Coimbra, Portugal
[++] Department of Biophysics, University of Bucharest, Bucharest, Romania

Received: March 7, 1994
Final version: May 6, 1994

Abstract
Amperometric detection using the batch injection analysis technique has been studied and compared with the current obtained at the wall-jet electrode under similar conditions using the oxidation of potassium ferrocyanide and the injection of samples of volume 10 to 100 μL. The form of the current transients has been analyzed and compared with the steady-state response at wall-jet disk electrodes. Good agreement is found at high dispension rate, differences at lower dispension rates being ascribed to radial diffusion effects. The importance of tip–electrode distance and injection volume have been evaluated; it is shown that the optimum distance is 3 mm and that maximum sensitivity requires a minimum injection volume of 14 μL. A detection limit of 50 μM using simple amperometric detection is estimated. Implications of these results for the efficient application of amperometric batch injection analysis are discussed.

Keywords: Batch injection analysis, Wall-jet electrode, Automated analysis, Hydrodynamic amperometry

1. Introduction

Batch injection analysis (BIA) is a newly developed analytical technique which involves the injection of small volumes of an analyte in solution from a micropipette tip onto the surface of a suitable detector placed a short distance away [1]. The response to the injection is in many ways similar to flow injection analysis (FIA) [2], except that in the case of BIA there is no continuously flowing carrier solution [3]; nevertheless, the washout characteristics of BIA enable consecutive experiments to be performed without memory affects. Applications to electrochemical detection, both amperometric [1, 4–6] and potentiometric [7], have been described. The advantages of using programmable pipettes with a view to automation have been addressed [8]; these programmable pipettes allow a variety of dispension sequences and modes and are generally applicable to all types of BIA detection.

In the case of amperometric detection, where the tip is placed directly above the center of and perpendicularly to a disk electrode, the configuration is very similar to that of a wall-jet disk electrode system. In a wall-jet a fine, circular jet of fluid strikes a plane surface perpendicularly and spreads out radially over that surface [9]. The fluid which reaches the surface can only come from the incoming jet and not from any recirculation within the cell; this ensures that fresh incoming solution reaches the detector at all times. Thus, the cell size is unimportant. Wall-jet electrodes have often been applied to electroanalysis in flowing solution (see, e.g., [10]). The use of large volume cells can lead to greater ease of manipulation: they have been used for high performance liquid chromatography detection [11–13] and for studies of transport properties and mechanism (see, e.g., [14]).

In batch injection analysis, if the injection occurs over a sufficiently long period of time, then a steady-state current at the disk should be achieved and which should have the same value as that obtained at a wall-jet disk electrode under the same system geometry and experimental conditions.

It is the purpose of this article to evaluate the form of the amperometric response at fixed potential in BIA and to compare the results obtained in BIA with those at the wall-jet disk electrode under similar, steady-state conditions.

2. Experimental

Experiments were carried out in a large wall-jet cell constructed from perspex described previously [10], modified such that the inlet section was replaced by a tapered hole into which the micropipette tip fitted exactly. The tip was placed over the center of a platinum disk electrode (radius 1.64 mm), the electrode-tip distance being regulated by screwing the disk electrode assembly in and out. The electrode was polished with diamond lapping spray down to 1 μm particle size before each series of experiments. A platinum gauze counter electrode and saturated calomel reference electrode (SCE) were employed. The cell is shown in Figure 1.

A programmable motorized electronic micropipette (EDP-Plus EP-100, Rainin Instrument Co. Inc.) was used for performing the injections. This permits injections in the range from 10 μL–100 μL in increments of 0.1 μL. It is possible to programme the micropipette to perform consecutive injections and three dispensing speeds are available. Potentials were controlled and current data recorded with a PAR273A potentiostat using computer-controlled M270 Research Electrochemistry software.

Most experiments were carried out using an injecting solution of 2.0 mM potassium ferrocyanide in 0.4 M potassium sulfate electrolyte, prepared from analytical grade reagents and Millipore Milli-Q nanopure water. The cell was filled with potassium sulfate electrolyte. All experiments were performed at room temperature (25 ± 1 °C).

3. Results and Discussion

The BIA response was evaluated using the oxidation of potassium ferrocyanide in potassium sulfate electrolyte, which

  1040-0397/95/0303-225 $ 5.00+.25/0

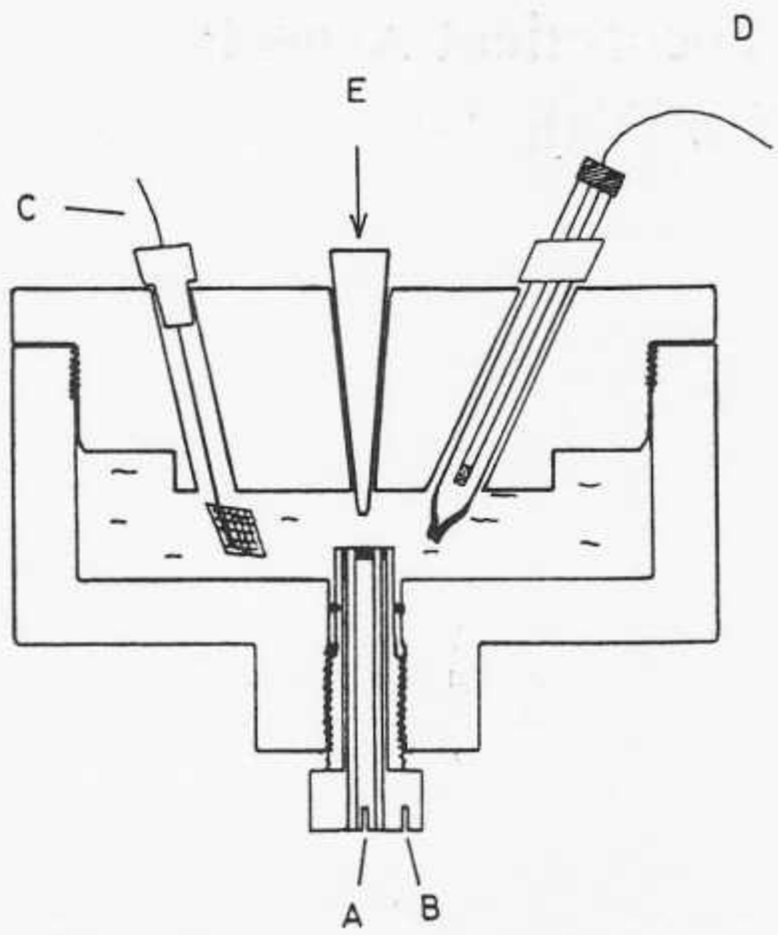

Fig. 1. Scheme of cell used for BIA amperometric measurements. A: disk electrode; B: ring electrode; C: auxiliary electrode; D: SCE reference electrode; E: micropipette tip. Cell constructed of perspex.

exhibits fast electrode kinetics at platinum electrodes and for which $E_{1/2} = 0.225$ V (vs. SCE) [10]. Most of the results to be presented were obtained at a fixed potential of +0.6 V (vs. SCE) to ensure that the current response is in the limiting current region.

A typical current transient for the highest flow rate is illustrated in Figure 2a. This shows that the transient can be divided into three regions, see Figure 2b: an initial portion until $t = t_1$ where the current rises almost linearly from zero to its maximum value, I_{max}; a second portion from $t = t_1$ until $t = t_2$ where the current is virtually constant at I_{max}, and a relaxation portion for $t > t_2$, after the injection period has ended.

In many injection experiments involving BIA (or FIA) a steady state is not achieved and dispersion is required to react with an added reagent. However, in this type of BIA experiment a property deriving from the composition of the original sample is being measured: dispersion hardly occurs and, as can be seen from Figure 2a, maximum sensitivity is reached at the steady-state. In FIA a constant response during a period of time does not often occur, and is confined to situations where injected volumes are sufficiently large and only small dispersion occurs – as for BIA application is to the measurement of parameters involving the composition of the original sample [15].

The micropipette dispension rates (i.e., volume flow rates) were calculated by measuring the time from where the transient began up until the end of the plateau of maximum current. The values were found to be 75.3, 47.6 and 24.5 μL s^{-1}, which agree with the manufacturers' data, taking into account the precision of their values.

3.1. Tip–Electrode Distance

The inlet nozzle–electrode distance is an important parameter in wall-jet studies [16], which is the tip–electrode distance in BIA. It is found at wall-jet electrodes that the current is less than its maximum value at very small inlet-electrode distances, rising to a maximum which is in agreement with the theoretical wall-jet equations at distances of 2–3 mm, and then decaying slightly at greater distances. This can be explained by the wall-jet hydrodynamics. For small distances the wall-jet profile cannot be followed due to back-wall effects. At large distances there is some dispersion of the jet of fluid and, if the incoming fluid differs slightly in viscosity in relation to that within the cell, then there can be break-up of the jet. We thus expect some dependence on tip–electrode distance in BIA.

The experimental results obtained are shown in Figure 3, illustrating the same tendencies as at wall-jet electrodes, more accentuated at the lowest dispension rate (i.e., lowest injection flow rate), where the streamlines stretch further back from the electrode surface. From these results a distance of 3 mm was chosen for use in all subsequent experiments.

3.2. Comparison With Wall-Jet Limiting Current

The limiting current at the wall-jet disk electrode, $I_{L,D}$, is given by [17]

$$I_{L,D} = 1.43\, nFR_1^{3/4} V_f^{3/4} D^{2/3} \nu^{-5/12} a^{-1/2} c_\infty \qquad (1)$$

where R_1 is the disk electrode radius, V_f is the volume flow rate of solution, D the diffusion coefficient of electroactive species of bulk concentration c_∞, ν the solution viscosity and a the jet diameter. Thus, if the potential applied to the electrode is in the

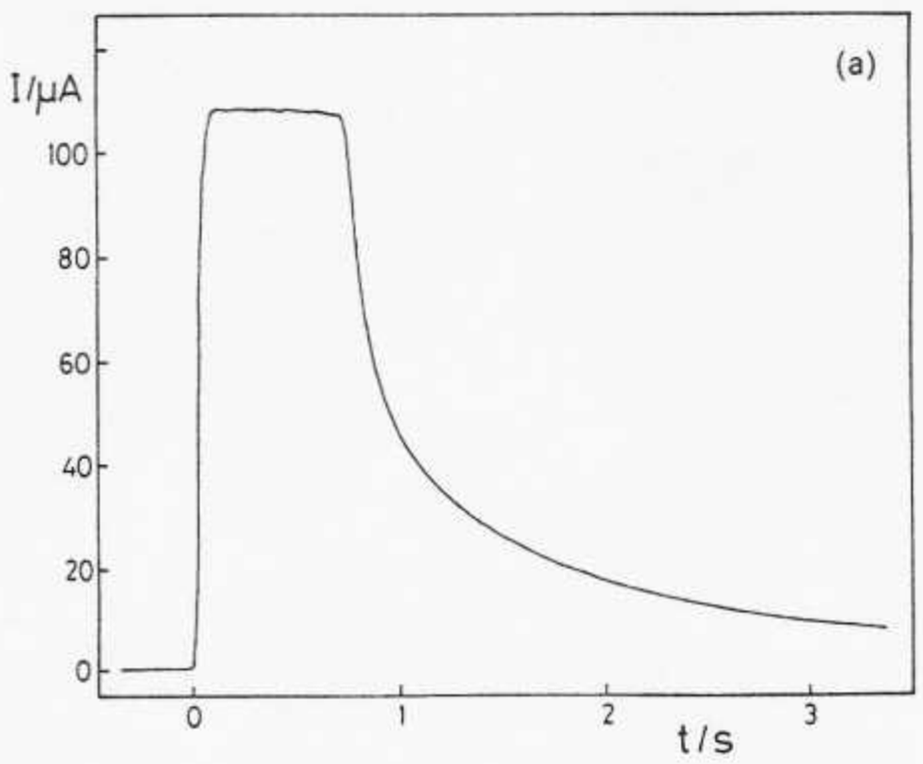

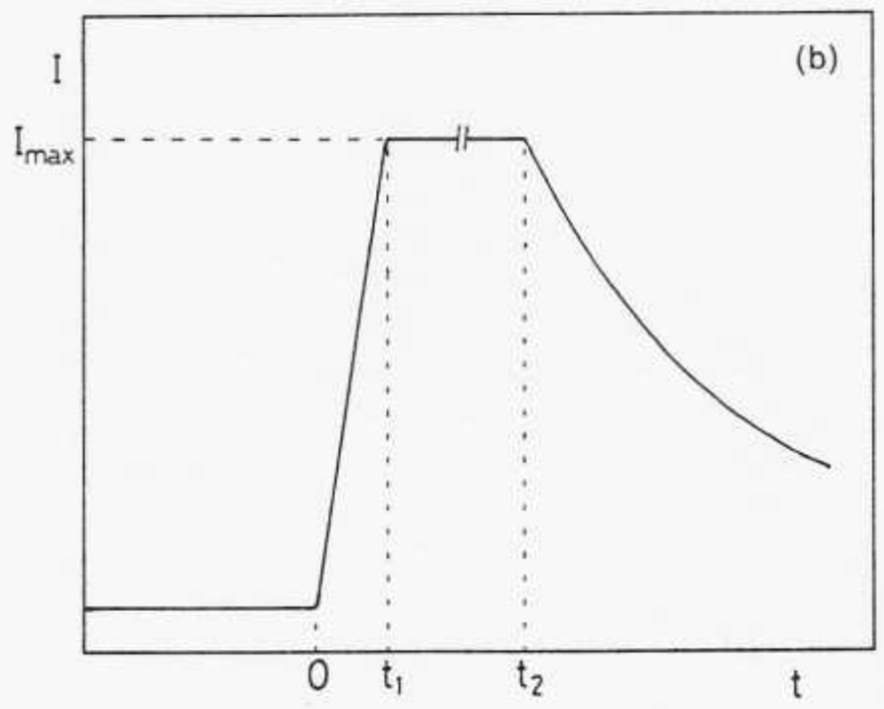

Fig. 2. a) Typical BIA transient at a flow rate of 75.3 μL s^{-1}, for injection of 60 μL of a solution of 2.0 mM $K_4Fe(CN)_6$ in 0.4 M K_2SO_4 electrolyte. b) Schematic of BIA transient showing division into three sections.

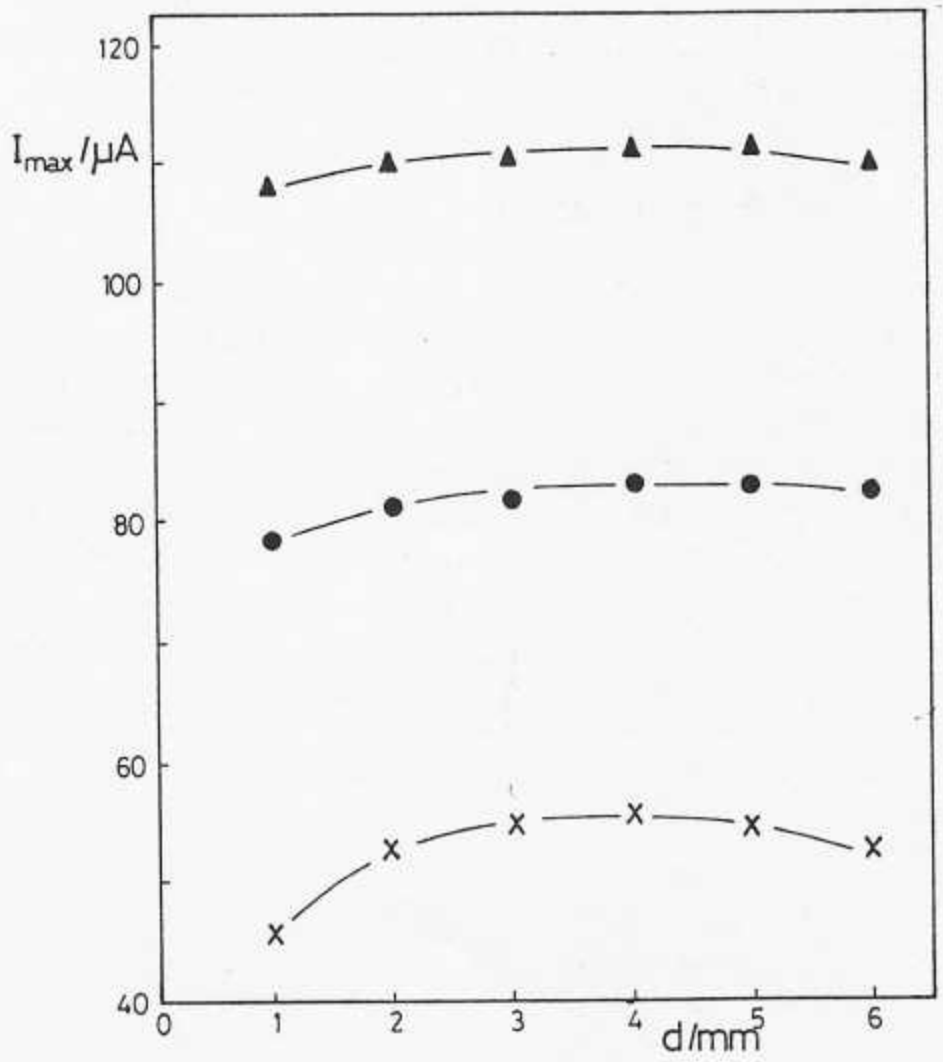

Fig. 3. Dependence of I_{max} on tip–electrode distance for the three flow rates: × 24.5, ● 47.6, ▲ 75.3 μL s^{-1}. Experimental conditions as Figure 2.

limiting current region, the plateau current, I_{max}, in BIA should be equal to $I_{L,D}$ and there should be a linear relation between I_{max} and $V_f^{3/4}$ (see below). This is indeed found as shown in Figure 4b. Substituting values for the cell geometry and for potassium ferrocyanide in potassium sulfate electrolyte of $D = 0.62 \times 10^{-5}$ cm^2 s^{-1} and $\nu = 0.94 \times 10^{-2}$ cm^2 s^{-1} [10], the value of the slope as predicted from the limiting current equation is

$$I_{L,D}/V_f^{3/4} = 7.860 \times 10^{-4}\,\mathrm{A\,(s/cm^3)^{3/4}} \qquad (2)$$

The experimental slope is less than this and has a negative intercept. However, there is good agreement between the limiting current equation and experiment at the highest flow rate. The higher currents obtained at lower flow rates suggests that the contribution of radial diffusion to the total mass transport should be taken into account, which will tend to increase the measured current: radial diffusion is neglected in the deduction of the limiting current equation presented above. Such a conclusion has been reached previously in experiments involving wall-jet electrodes [10, 18]. The flow rate above which there ceases to be an effect was shown to be approximately 50 μL s^{-1}, which approximately coincides with the medium flow rate.

These deductions are corroborated by data obtained at a concentric ring wall-jet electrode, see the lower line in Figure 4b. The limiting current expected at this electrode, $I_{L,R}$, is related to the limiting current at the disk electrode by

$$I_{L,R}/I_{L,D} = (R_3^{9/8} - R_2^{9/8})^{2/3}/R_1^{3/4} \qquad (3)$$

where R_2 is the inner ring radius and R_3 the outer ring radius. With the values of $R_1 = 1.64$ mm, $R_2 = 1.75$ mm and $R_3 = 1.89$ mm, the ratio of ring to disk currents is predicted to be 0.21. This is verified at the highest flow rate. At lower flow rates this ceases to be the case due to the radial diffusion contributions as discussed above. However, the ratio of the experimental slopes is 0.21.

These comparisons show that in order to apply the wall-jet limiting current equation to BIA measurements without recourse to calibration plots, the highest flow rate should be employed in order to be certain that radial diffusion does not contribute to the total measured current.

3.3. Effect of Injection Volume

It is clearly important that the current plateau is reached so that the highest sensitivity is achieved, and for which there must be a minimum injection volume. The effect of the injection volume is also shown in Figure 4a, and which suggests that the minimum volume is greater than 10 μL. However, plots such as those of Figure 5 are much more elucidative – here are plotted the total injection time and the time interval corresponding to the current plateau as a function of injected volume. Straight

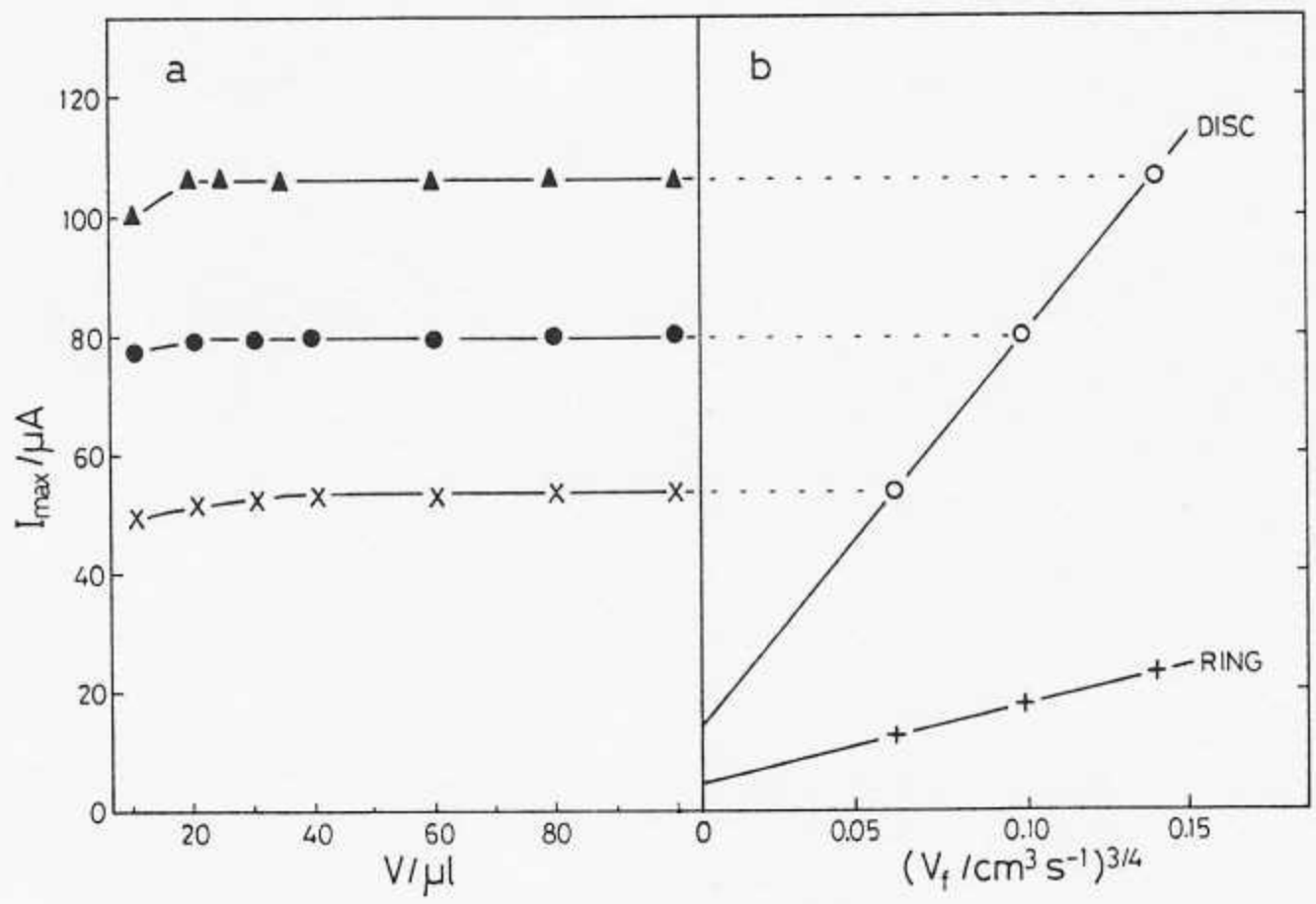

Fig. 4. Dependence of I_{max} on (a) injected volume, V, and (b) on volume flow rate as $V_f^{3/4}$. Experimental conditions as Figure 2.

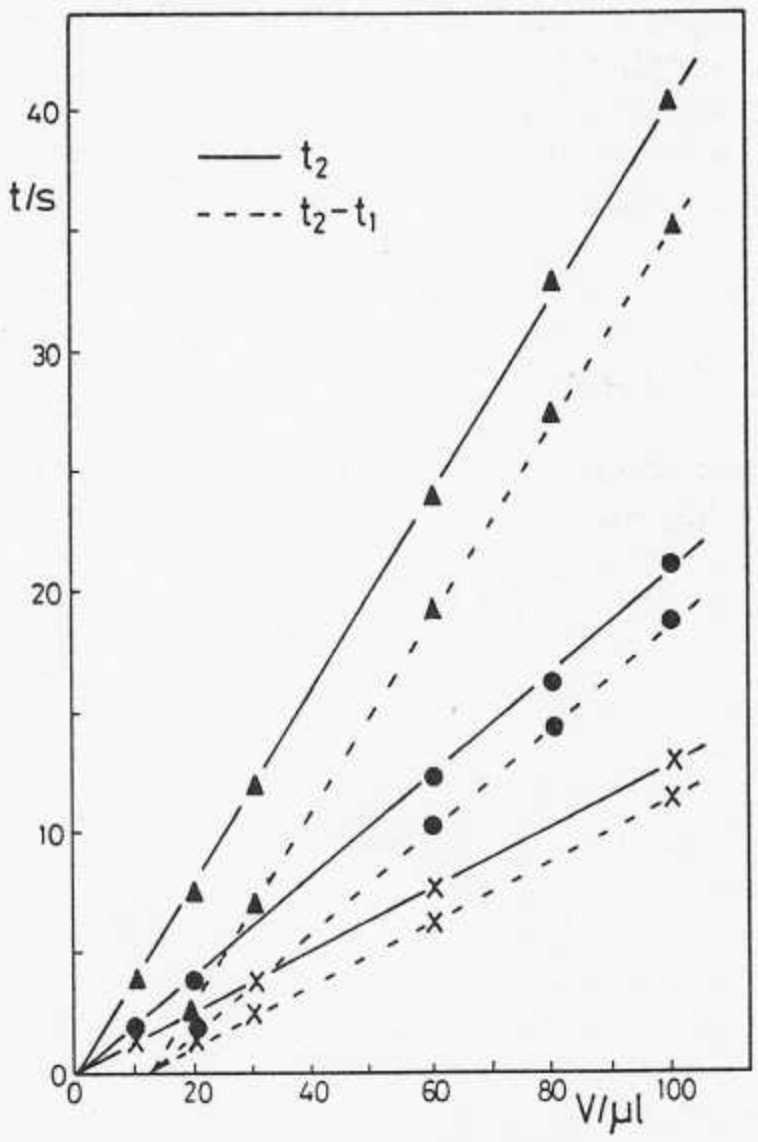

Fig. 5. Plots of t_2 and $(t_2 - t_1)$ vs. V for the three flow rates: × 24.5, ● 47.6, ▲ 75.3 μL s^{-1}. Experimental conditions as Figure 2.

lines are obtained, and the intercepts of the latter plots are 12.1, 12.5 and 13.2 μL for the three flow rates in ascending order, which corresponds to the minimum volume necessary to reach the plateau current and thus achieve maximum sensitivity. Thus in practice, the minimum practical injection volume is 14 μL, which implies that for a total volume of 100 μL it should be possible to perform 7 consecutive injections. Note that for an electroactive species exhibiting slower electrode kinetics, the minimum injection volume necessary to reach the plateau will be greater.

Other considerations to be borne in mind are the repeatability and reproducibility of the determinations. These were tested for volumes of $\geq 15\,\mu$L. Six consecutive injections gave a relative standard deviation of 0.9%, which leads to a detection limit, defined as 3σ, at $\sim 50\,\mu$M, which was verified experimentally.

Also tested was the injection of the sample without supporting electrolyte. Good results were obtained without deviation from the response in excess supporting electrolyte, but the noise level was slightly higher. This can be contrasted with the results of Gunasingham et al. [12] who found a decrease in the peak height at a wall-jet detector of a factor of ten in the determination of estrogens by HPLC using precolumn injection and without addition of electrolyte, correctly attributed by them to the increased ohmic drop between working and reference electrodes. Two reasons for these differences can be advanced. First, in [12] the eluent containing the previously injected species entered the cell over a period of minutes creating a large zone without added electrolyte near the working electrode; in the BIA case the injection is directly into the cell and has a maximum volume of 100 μL. Second, but less importantly, a higher concentration of supporting electrolyte was used in the main cell body in our case (0.4 M compared to 0.05 M). Thus in the amperometric BIA experiments described here the increased ohmic drop is negligible, which has important implications for the analysis of real samples in that pre-addition of electrolyte becomes unnecessary.

3.4. Current Decay Transient

We now turn to the decay portion of the curve. This is different from a chronoamperometric transient due to a change in potential both in unstirred solution, which follows the Cottrell equation, and is also different from the transient obtained at the wall-jet electrode under steady-state flow conditions [10]. In fact, both the current rise at the beginning of the transient and the current decay are due to concentration steps. The variation of current with time in the initial portion of the transient (positive concentration step) and in the current decay (negative concentration step) is qualitatively similar to the variation of potential with time on stepping the primary ion activity at an ion-selective electrode with solution impinging in a wall-jet fashion [19], where it was found that diffusion is the dominating process.

A log–log plot constructed from the experimental points of two transients, one at the highest and the other at the lowest flow rates, is shown in Figure 6. From the initial $t^{-1/2}$ dependence it would appear that the convection from the injection period stops very rapidly. At the beginning of the current decay the wall-jet electrode is covered with injected solution, so that this time dependence is not unexpected, and is similar to a conventional Cottrell-type response. We then recognize that the depletion of the diffusion layer takes place due to both reaction at the electrode surface and due to diffusion into bulk solution which contains little or no electroactive species. Thus the current decays more rapidly, in fact tending to a $1/t$ relationship as shown in the plots. Analysis of a large number of plots shows that this behavior is similar at all three flow rates.

4. Conclusions

A number of novel aspects have been shown by this work, which extends the use of programmable micropipettes for amperometric detection in BIA as introduced in [8]. We have shown that the current during the larger part of the injection period is very similar to that obtained at a wall-jet electrode under steady-state conditions. In particular, at the highest flow

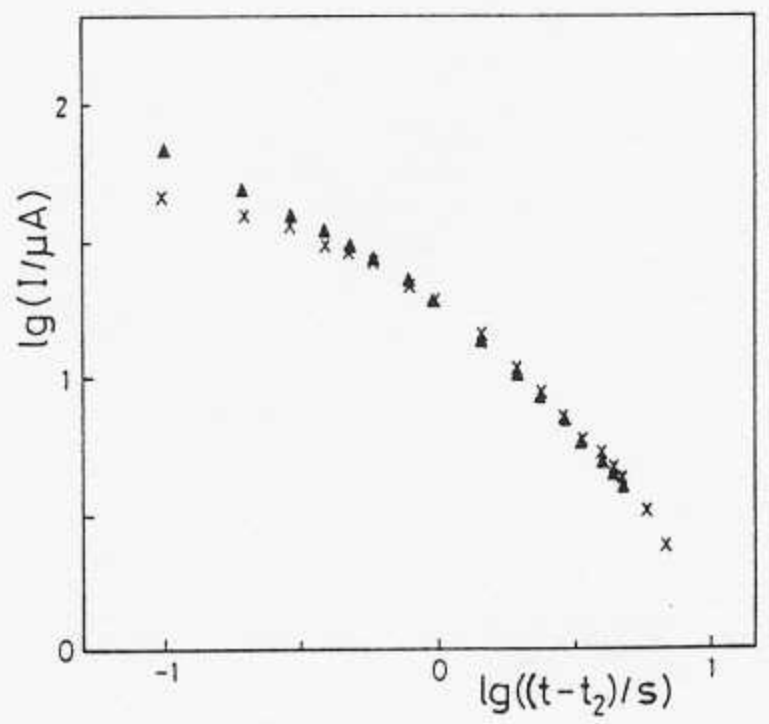

Fig. 6. Plot of lg I vs. lg $(t - t_2)$ for the current decay portion of two transients at flow rates × 24.5, and ▲ 75.3 μL s^{-1}.

rate where radial diffusion can be neglected, the wall-jet electrode equations can be used for concentration determination from the analysis of the plateau current in addition to or as an alternative to the construction of calibration plots. The importance of using a minimum injection volume to ensure that the plateau current is reached, resulting in maximum sensitivity, has been discussed as well as the choice of an appropriate tip–electrode distance of ~3 mm. This minimum injection volume can be conveniently and simply determined from plots of time interval for the steady-state plateau current vs. injection volume.

With these parameters determined, the technique offers an accurate and highly sensitive way of determining small quantities of analyte, combining the advantages of wall-jet-type electrode detection and injection techniques.

5. Acknowledgement

One of us (L.C.-M.) wishes to thank the Tempus programme of the European Community (JEP Contract No. 4223-92/1) for a study grant.

6. References

[1] J. Wang, Z. Taha, *Anal. Chem.* **1991,** *63*, 1053.
[2] J. Ruzicka, E.H. Hansen, *Flow Injection Analysis*, 2nd ed., Wiley, New York, **1988**.
[3] J. Wang, *Microchem. J.* **1992,** *45*, 219.
[4] L. Chen, J. Wang, L. Angnes, *Electroanalysis* **1991,** *3*, 773.
[5] J. Wang, J. Lu, L. Chen, *Anal. Chim. Acta* **1992,** *259*, 123.
[6] A. Amine, J.-M. Kauffmann, G. Palleschi, *Anal. Chim. Acta* **1993,** *273*, 213.
[7] J. Wang, Z. Taha, *Anal. Chim. Acta* **1991,** *252*, 215.
[8] J. Wang, L. Chen, L. Angnes, B. Tian, *Anal. Chim. Acta* **1992,** *267*, 171.
[9] M.B. Glauert, *J. Fluid Mech.* **1956,** *1*, 625.
[10] C.M.A. Brett, A.M. Oliveira Brett, A.C. Fisher, R.G. Compton, *J. Electroanal. Chem.* **1992,** *334*, 57.
[11] H. Gunasingham, *Anal. Chim. Acta* **1984,** *159*, 139.
[12] H. Gunasingham, B.T. Tay, K.P. Ang, *Anal. Chem.* **1984,** *56*, 2422.
[13] L.J. Nagels, J.M. Kauffmann, C. Dewaele, F. Parmentier, *Anal. Chim. Acta* **1990,** *234*, 75.
[14] C.M.A. Brett, A.M. Oliveira Brett, J.L.C. Pereira, *Electroanalysis* **1991,** *3*, 683.
[15] D. Betteridge, *Anal. Chem.* **1978,** *50*, 832A.
[16] W.J. Albery, C.M.A. Brett, *J. Electroanal. Chem.* **1983,** *148*, 211.
[17] J. Yamada, H. Matsuda, *J. Electroanal. Chem.* **1973,** *44*, 189.
[18] R.G. Compton, A.C. Fisher, M.H. Latham, R.G. Wellington, C.M.A. Brett, A.M. Oliveira Brett, *J. Appl. Electrochem.* **1993,** *23*, 98.
[19] T.R. Berube, R.P. Buck, E. Lindner, K. Toth, E. Pungor, *Anal. Chem.* **1991,** *63*, 946.